Journal of Engineering Physics and Thermophysics, Vol. 67, Nos. 5-6, 1994

ROLE OF END FLOWS IN THE INTERNAL AERODYNAMICS OF VORTEX PLASMATRONS

N. A. Kostin, A. S. Olenovich, L. P. Podenok, and L. I. Sharakhovskii

UDC 533.915:533.6

The important role of boundary layers on the end walls of the supply vortex chamber and a dead-end tubular electrode in the formation of the entire flow field in a plasmatron is shown by experimental investigations using the method of laser anemometry. Formulas are proposed that enable one to take into account the influence of flows along these layers on the tangential velocity field of a gas vortex flow.

High energy parameters of vortex plasmatrons are ensured mainly by their internal aerodynamics, which forms the character of the interaction of the arc discharge with the gas flow. Some researchers have long drawn attention to the important role of end boundary layers in vortex apparatuses that are similar aerodynamically to plasmatrons. Thus, in [1–3] this is noted concerning the formation of the flow field in short vortex chambers, in which the height-to-radius ratio is smaller than unity ($H/R_0 < 1$) and in which practically the entire flow rate may go to the end boundary layers, which form the entire flow field in the chamber. A substantial influence of end flows is noted in long vortex chambers ($H/R_0 > 1$) as well in [4]. In particular, an increase in the roughness of the end wall caused a displacement of the tangential velocity maximum in a cyclone to a larger radius. End effects are most completely described in [5] theoretically and phenomenologically. However, no existing theoretical models for calculating vortex chambers enable us to take account of the influence of the secondary flows and tangential velocity losses on the periphery that can be caused by these flows [5–8]. The special features of the flow caused by end effects are most characteristic of vortex chambers of plasmatron interelectrode inserts, in which intense twisting of the flow occurs for limited gas flow rates and which decrease the efficiency of discharge stabilization. Furthermore, the problem of the possible use of end effects to control vortex flow in a plasmatron as a whole is currently of concern but is hardly investigated as yet.

From the aerodynamic viewpoint we can consider a vortex plasmatron as a combination of two vortex chambers: a short supply chamber with the characteristic height H (see Fig. 1) and a long one (an electrode) with the characteristic height L. The influence of near-end flows on the aerodynamics of these chambers has special features considered below.

For a number of reasons, one of which is the need to place interelectrode electric insulation outside tubular electrodes, the radius of the supply vortex chamber of a plasmatron is usually considerably larger than the internal radius of the tubular electrodes. This is important since it leads to the appearance of a radial velocity component over a considerable stretch of the chamber, which plays a large part in the formation of the entire vortex flow field. It is usually assumed that in such flows the tangential velocity fields are described satisfactorily by the formula for a quasipotential vortex:

$$VR^a = \text{const} \quad (a < 1). \tag{1}$$

In short vortex chambers a characteristic feature of the flow throughout the entire volume except the near-axis region is a negligibly small value of the axial velocity. In a near-axis region whose radius is similar to the internal radius of the electrode a noticeable axial velocity appears and the gas rotation becomes similar to a quasisolid one.

Academic Scientific Complex "A. V. Luikov Institute of Heat and Mass Transfer," Minsk. Translated from Inzhenerno-Fizicheskii Zhurnal, Vol. 67, Nos. 5-6, pp. 392-399, November-December, 1994. Original article submitted July 20, 1993.

1062-0125/94/6756-1031$12.50

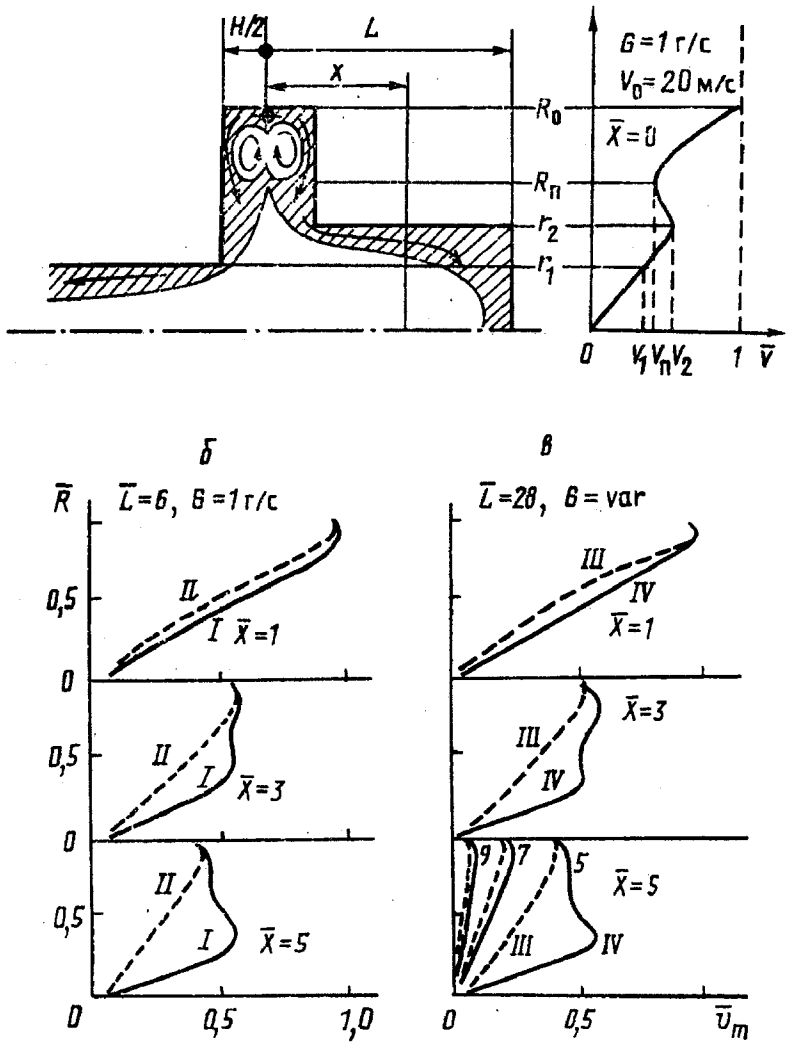

Fig. 1. Scheme of flows in boundary layers (hatched) inside a plasmatron and tangential velocity profiles: a) in the twist cross section; b, c) at different distances from it into the depth of the dead-end electrode; *I*) a smooth end wall, v_1^{max} = 8.6 m/sec; *II*) an end wall with microirregularities, v_1^{max} = 8.4 m/sec; *III*) G = 1 g/sec (Re $r_2/r_1 = 1.1 \cdot 10^3$), v_1^{max} = 19 m/sec.

Results of investigating the internal aerodynamics of vortex plasmatrons using a laser Doppler velocity meter (LDVM), which ensures high accuracy for measurements and the absence of a disturbing action on the flow, are presented below. These measurements were performed on transparent plasmatron models in the absence of an electric arc. Furthermore, in a series of regimes we performed control experiments on natural electric arc plasmatrons without using an LDVM so as to compare parameters of the discharge for different plasmatron aerodynamics.

Investigations using an LDVM enabled us, in particular, to establish the reason why even a considerable increase in the inlet velocity of the gas produced by decreasing the cross section of the supply channels of the vortex chamber does not result in any substantial intensification of the twisting in the electrodes. For example, in an experiment with a vortex chamber with a radius of 45 mm a twelvefold (from 5.3 to 64 m/sec) increase in the inlet velocity led to an increase in the tangential velocity at the electrode radius (10 mm) by just a factor of 1.4 (from 6.5 to 9.4 m/sec). This cannot be explained by local loses at the inlet to the chamber alone [9].

Visualization of the flow by introducing smoke into the flow and using a thin flat beam of light, a so-called "light knife," showed that with a large tangential velocity and a limited flow rate the bulk of the gas goes to the boundary layers on the end walls immediately at the periphery and then flows along them to the outlet from the

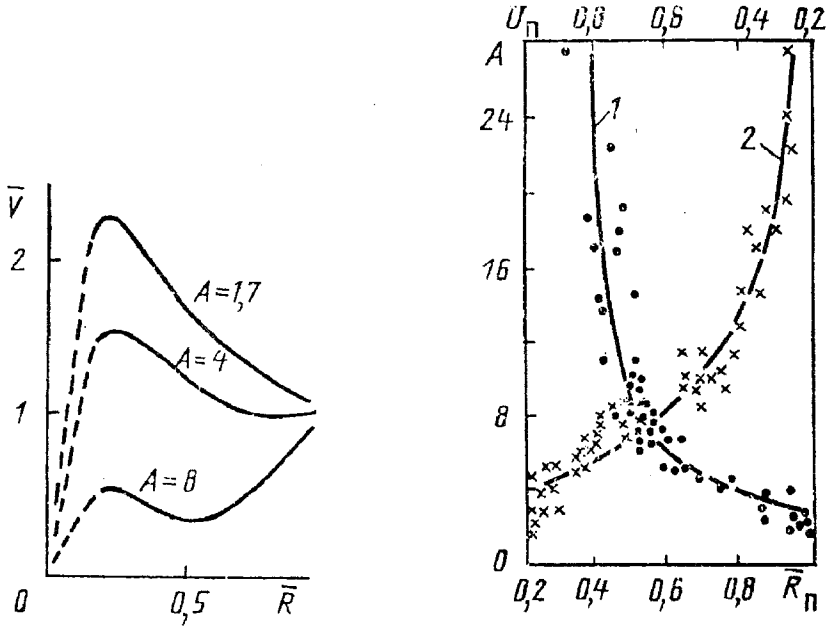

Fig. 2. Dimensionless profiles of the tangential velocity in a vortex chamber ($\bar{V} = V/V_0$).

Fig. 3. Radius of the potential core of a vortex flow and twisting rate at its boundary vs the parameter A: 1, 2) by formulas (3) and (4), respectively.

chamber. Until the boundary layers on the opposite walls join, the radial velocity of the flow in the middle cross section of the chamber may equal zero and even be negative (the zone of reverse currents). In the zone occupied by reverse currents we observe a drop in the tangential velocity rather than a growth, as should have been the case according to (1). The external radius of the quasipotential region, where relation (1) is obeyed, in this flow coincides approximately with the internal radius of the reverse current zone. The size of the reverse current zone increases as the chamber's geometric parameter R_0^2/F increases and decreases with increasing flow rate. Figure 1 presents schematically the flow in the described regime and the corresponding tangential velocity profile in the vortex chamber. Therefore, to use (1) in calculating the plasmatron vortex chamber, we first need to determine the radius of the quasipotential region of the vortex flow, which can be much smaller than the vortex chamber radius ($R_p < R_0$). The existing theoretical models, as has been mentioned above, do not enable us to calculate this radius with account for the above special features: the secondary flows and drop in the tangential velocity at the periphery.

In this connection generalization of experimental data on vortex flows using a parameter that takes into account the influence of the end effects can be promising. A parameter of boundary layer interaction proposed in [1] and characterizing the fraction of the total flow rate in the vortex chamber that flows through the end boundary layers was found to be appropriate for this purpose. In a modified form it can be written as

$$A = 1.68R_0^2\varepsilon^{0.8}/\mathrm{Re}^{0.2}F. \tag{2}$$

Here Re is calculated from the mass-mean velocity in the supply channels and the vortex chamber radius.

Processing of extensive experimental material [9, 10] on this parameter showed that the described special features of the flow regimes can be generalized satisfactorily with its aid. Figure 2 gives dimensionless tangential velocity profiles in vortex chambers that illustrate the influence of the parameter A. From the figure it can be seen that for $A = 8$ the radius of the quasipotential zone amounts to only half the chamber's radius. If we use relation (1) without taking this into account, the error in calculating the tangential velocity at the electrode radius can be large (100% or more).

Figure 3 gives results of generalizing the radius of the vortex flow quasipotential zone R_p and the value of the tangential velocity at this radius as a function of A. For $\bar{R}_p$ we obtained the expression

$$\overline{R}_p = 1.16/(A - 1.2) + 0.36 \quad (\overline{R}_p \leq 1), \tag{3}$$

and for $\overline{V}_p$

$$\overline{V}_p = 4.69/(A + 1.08) + 0.08 \quad (\overline{V}_p \leq 1). \tag{4}$$

In generalizing $\overline{R}_p$ and $\overline{V}_p$ in the form of (3) and (4) use was made of the expression for ε in [11] with the constraint $\varepsilon \leq 1$:

$$\varepsilon = 20\,(F/2\pi R_0 H)^{0.68}. \tag{5}$$

The root-mean-square deviation of experimental points with respect to (3) and (4) amounted to about 15%.

At $A = 3$ $\overline{R}_p \approx 1$, $\overline{V}_p \approx 1$, i.e., the quasipotential zone radius coincides with the chamber radius R_0. With $3 \leq A \leq 4$ $\overline{V}_p = 1.0$ and $\overline{R}_p < 1$, which reflects the presence of a zone of constant velocity, equal to εV_{inl}, in the portion from R_0 to R_p at the periphery. With $A > 4$ $\overline{R}_p < 1$ and $\overline{V}_p < 1$, i.e., a zone of drop in tangential velocity appears at the periphery of the chamber [9].

To calculate a in formula (1), we can use an empirical expression that is valid in the range $0.3 \leq a \leq 0.8$ [12]:

$$a = 1.14\,[\log\,(G/2\pi\mu AH)]^{0.38} - 1. \tag{6}$$

The value of the parameter A in this formula is calculated from the values of R_p and V_p if at least one of them is smaller than 1.

As is known from theoretical calculations using different models, the intensity of twisting has a slight effect on integral electric characteristics of an arc discharge. It has the strongest effect on the distribution of gasdynamic parameters along the radius of the channel [13, 14]. When high local values of enthalpy are needed, it can be appropriate to use intense twisting that causes movement of a considerable mass of gas to peripheral zones of the flow with a simultaneous increase in the near-axis enthalpy, its decrease at the periphery, and an increase in thermal efficiency. As has already been mentioned, from the viewpoint of the aerodynamics of vortex chambers it is the twisting of the flow in a discharge channel of a sectional interelectrode insert of a plasmatron with distributed gas supply that is most difficult to intensify, which restricts its potentialities in attaining peak values of the flow enthalpy. This is explained by unsatisfactory aerodynamic characteristics of vortex chambers because of sharing of the discharge between a large number of chambers. The latter imposes constraints on Re and F in relation (2) by increasing the value of the parameter A and diminishing the twisting.

We performed experiments with an improved interelectrode insert, in which, to decrease the parameter A, we introduced intentionally an excessive gas discharge at small radii R_0 similar to the channel radius, with subsequent partial suction from the boundary layer, distributed along the insert length. It was assumed that the intense field of centrifugal forces and lamination of the flow should decrease radial diffusion of the enthalpy from the near-axis zone to the channel walls. Indeed, on this plasmatron we obtained an axial enthalpy of the flow of up to 45 MJ/kg with 85–90% thermal efficiency and a working pressure of 2.5–3.5 MPa [15]. We calculated the enthalpy of the flow by the Fay–Riddel equation from heat fluxes measured using nonstationary calorimeters. This method enjoys wide use in high-enthalpy gas flows, for example, in hypersonic wind tunnels [16].

Investigations using an LDVM also established the important role of the end boundary layer in the formation of the flow field in a dead-end electrode. Figure 1 shows schematically the flow in a vortex plasmatron with tubular dead-end and through electrodes. The flow from the boundary layers on the end walls of the supply vortex chamber enters the electrodes. In the dead-end electrode the flow turns around on the end wall and forms a near-axis return flow directed toward the outlet. The distribution of discharges between the electrodes, as investigations using an LDVM show, is determined by the ratio of their radii: an increase in r_2 compared to r_1 causes an increase in the fraction of the discharge through the dead-end electrode. As will be shown later, the electrode length, which determines the degree of influence of the boundary layer at the rear end wall on the formation of the vortex flow field depends, has a very strong effect on the velocity field in this electrode.

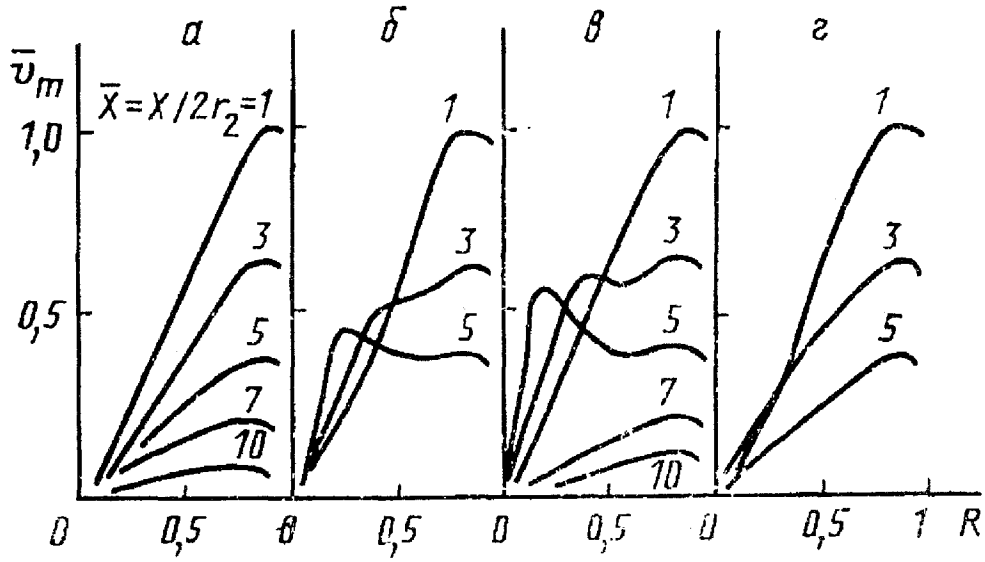

Fig. 4. Tangential velocity profiles in a dead-end electrode (r_1 = 22 mm, r_2 = 36 mm): a, b, d) G = 1 g/sec; c) 2; a, b) $\bar{L}$ = 28; c, d) $\bar{L}$ = 6.

Figure 4a and b presents a comparison of the tangential velocity fields in the dead-end electrode for $\bar{L}$ = 28 and $\bar{L}$ = 6, from which we can clearly see the influence of the end wall. Whereas at $\bar{L}$ = 28 there is gradual damping of the twisting along the electrode length with the shape of the profiles preserved, at $\bar{L}$ = 6, as the end wall is approached, the shape of the profiles changes considerably: a near-axis maximum of tangential velocity appears on them. Its appearance can be explained by convective transfer of angular momentum from the periphery to the axis by a radial flow that arises in the boundary layer on the end wall. The reason for the onset of this wall flow is common in the short vortex chamber and the long one. It is that the balance between the radial pressure gradient and centrifugal forces in the boundary layer is disturbed owing to impeding of the twisting by frictional forces. Because of weakened centrifugal forces it is the radial pressure gradient that prevails here. This causes intense mass transfer to the axis of the flow along the boundary layer on the end wall with simultaneous transfer of some angular momentum to the axis, which causes a local increase here in the twisting rate of the flow.

At an increased flow rate and a sufficient length of the dead-end electrode a gas "quasiwall" forms abruptly in a certain cross section of the dead-end electrode: a localized turning zone, in which the flow separates suddenly from the cylindrical surface of the electrode and, stopping short of reaching the electrode end, turns around and flows to the axis and then in the opposite direction, forming a flow similar to that along the end wall. Measurements show that immediately behind this cross section the twisting rate abruptly decreases several fold (2–3 times or more). This can be seen clearly from Fig. 4c, where the twisting rate decreases abruptly between $\bar{X}$ = 5 and 7. The axial pressure gradient on the electrode wall (measured by a water micromanometer) is found to be vanishingly small in passing through the above cross section. This demonstrates virtual absence of longitudinal flow of the gas behind the local turning zone. Our investigations using an LDVM established that formation of the local turning zone always takes place with the value of the parameter $\mathrm{Re}\, r_2/r_1 = 5.5 \cdot 10^3$ ($\mathrm{Re} = \rho u_1 r_1/\mu$). For the axial coordinate of the local turning zone we obtained, by generalizing the experimental results, the following expression:

$$\bar{X} = 9.1 - 18.2/(V_1/u_1 + 2)\,. \qquad (7)$$

With $r_2 > r_1$ we calculate V_1 from V_2, taking into account that with $r > r_2$ quasisolid rotation of gas (V/r = const) is observed. We calculate V_2 according to formulas (1)-(6) (as well as V_1 in the case $r_2 = r_1$). The root-mean-square deviation of experimental points from the dependence determined by (7) did not exceed 5%. If the end wall of the electrode is no farther than 5–6 diameters behind the cross section determined by (7), the local turning zone goes over to the wall. This is not observed if the end wall has considerable microirregularities (about a quarter of the electrode radius). If the length of the dead-end electrode is smaller than or equal to the value determined by formula

(7), the presence of these microirregularities on the end wall alters profoundly the flow pattern in the dead-end electrode: the zone of quasisolid rotation expands in radius and propagates over the entire length of the dead-end electrode with total elimination of near-axis maxima of tangential velocity (Fig. 4d) irrespective of the value of the flow rate. We can explain this by suppression of convective transfer of angular momentum to the axis by the microirregularities on the wall. A further increase in the microirregularity height does not alter fundamentally the flow pattern but it causes increased losses of the twisting rate.

The character of evolution of the tangential velocity fields with movement into the depth of the electrode is seen most clearly by superimposing the profiles inherent in a short ($\overline{L} = 6$) electrode with a smooth or uneven end wall (see Fig. 1b) and in a long ($\overline{L} = 28$) electrode in the presence or the absence of the local turning zone, i.e., with Re $r_2/r_1 \lesssim 5.5 \cdot 10^3$ (see Fig. 1c).

Damping of twisting along the length of an electrode with the described macroirregularities on the end wall is generalized satisfactorily in dimensionless parameters (we measured v by the maximum on the velocity profile in each cross section):

$$\overline{v} = 0.104 \exp\left[113.6/(\overline{X}V_1 r_2^2/u_1 r_1^2 + 49.4)\right]. \tag{8}$$

The root-mean-square deviation of the experimental points from (8) amounted to about 9%. Experiments with an electric arc showed that its combustion stability increases substantially in this electrode, voltage pulsations decrease, and arc ties rotate more uniformly and with a larger average speed. This improves the thermal regime of the electrode and decreases its erosion. When an external magnetic field is applied, the arc ties are likely to be located in cross sections close to the solenoids, which enables us to control more reliably their position using the magnetic field. This can also be used to lower erosion [17]. In this case, however, it should be taken into account that the twisting rate for the flow decreases somewhat in the through electrode, particularly with a small length of the dead-end electrode. Thus, with a length of 2 diameters ($\overline{L} = 2r_2$) the rate of twisting in the through electrode decreases by one-half and with a length of 6 diameters by 30%. This has a slight effect on the operating regime of the through electrode since the dominant role in decreasing the local thermal loads is played here by longitudinal shunting of the arc discharge, which has a considerable frequency and span owing to the high axial velocity of the gas. This effect is absent altogether in plasmatrons with interelectrode inserts and distributed gas supply because of twisting of the flow by additional vortex chambers.

Therefore, in intense vortex flows confined by walls, which is characteristic of plasmatrons, boundary layers on the end walls of both the supply vortex chamber and the dead-end tubular electrode have a substantial effect on the formation of the entire flow field inside the discharge chamber of the plasmatron and on its characteristics. Control of the flow in the end boundary layers can be used to improve the characteristics of both plasmatrons and other technological vortex apparatuses.

NOTATION

H, vortex chamber height; R, R_0, current and external radii of the vortex chamber, respectively; R_p, $\overline{R}_p = R_p/R_0$, absolute and dimensionless value of the radius of the quasipotential region of the flow, respectively; r_1, r_2, radii of through and dead-end electrodes; F, total cross-sectional area of supply channels of the vortex chamber; V_{inl}, mass-mean velocity of gas in supply channels of the vortex chamber (inlet velocity); ε, coefficient of conservation of inlet velocity, which is equal to V_0/V_{inl} and takes into account input losses; $\overline{V} = V/V_0$, dimensionless tangential velocity at the radius in the vortex chamber; V_p, $\overline{V}_p = V_p/\varepsilon V_{inl} = V_p/V_0$, absolute and dimensionless value of the tangential velocity at the external boundary of the quasipotential region; V, V_0, V_1, V_2, tangential velocity of gas in the vortex chamber: the current value and values at the radii R_0, r_1, and r_2; v, $\overline{v} = v/V_2$, absolute and dimensionless value of the tangential velocity in the dead-end electrode; $\overline{v}_m = v/v_1^{max}$, where v_1^{max} is the tangential velocity maximum at $\overline{X} = 1$; u_1, mean-mass axial velocity in the through electrode; $\overline{X} = X/2r_2$, dimensionless distance from the twist cross section; L, $\overline{L} = L/2r_2$, absolute and dimensionless value of the dead-end electrode length; G, mass flow rate; μ, dynamic viscosity.

REFERENCES

1. M. L. Rozentsveig, V. S. Levellen, and D. G. Ross, Raketnaya Tekhn. Kosmonavtika, No. 12, 94-103 (1964).
2. D. N. Wormley, Teor. Osn. Inzh. Raschetov, No. 2, 145-149 (1969).
3. S. S. Kuok, Ngo Din T'yen, and Su Lin, Teor. Osn. Teplotekhn., No. 3, 181-188 (1972).
4. F. N. Saburov, Aerodynamics and Convective Heat Transfer in Cyclone Heating Devices [in Russian], Leningrad (1982).
5. S. S. Kutateladze, E. P. Volchkov, and V. I. Terekhov, Aerodynamics and Heat and Mass Transfer in Confined Vortex Flows [in Russian], Novosibirsk (1987).
6. I. I. Smul'skii, Aerodynamics and Processes in Vortex Chambers [in Russian], Novosibirsk (1992).
7. V. A. Zhigula and V. P. Koval', Prikl. Mekh., **11**, No. 9, 65-72 (1975).
8. M. A. Gol'dshtik, Vortex Flows [in Russian], Novosibirsk (1981).
9. L. I. Sharakhovskii and N. A. Kostin, in: Proceedings of the International School-Seminar "Heat and Mass Transfer in Plasmachemical Processe" [in Russian], Part 1, Minsk (1982), pp. 74-90.
10. V. K. Mel'nikov, E. P. Sukhovich, and V. A. Zavgorodnii, Izv. Akad. Nauk Latv. SSR, Ser. Fiz. Tekhn. Nauk, No. 3, 73-79 (1969).
11. V. A. Rudnitskii, Efficiency of Thermal-Power Processes [in Russian], Vladivostok (1979), Issue 1, pp. 126-133.
12. N. A. Kostin, "Optimization of the internal gasdynamics of vortex-design plasmatrons," Candidate's Dissertation, Minsk (1985).
13. L. I. Kolonina and V. Ya. Smolyakov, Generators of Low-Temperature Plasma [in Russian], Moscow (1969), pp. 209-218.
14. P. Z. Alimov and V. M. Islamov, Heat and Mass Transfer in Chemical Engineering [in Russian], Kazan' (1978), Issue 6, pp. 61-64.
15. L. I. Sharakhovskii, A. F. Klishin, A. S. Olenovich, and L. P. Podenok, Abstracts of Papers of the VIII All-Union Conference on the Physics of Low-Temperature Plasma [in Russian], Part 2, Minsk (1991), pp. 146-147.
16. J. H. Painter, AIAA Paper, No. 75-105, 11 (1975).
17. L. I. Sharakhovskii, A. S. Olenovich, L. P. Podenok, V. N. Borisyuk, and A. M. Yesipchuk, Inzh.-Fiz. Zh., 66, No. 6, 702-706 (1994).